Available online at www.sciencedirect.com
SCIENCE DIRECT
Polymer 47 (2006) 2539–2547
polymer
www.elsevier.com/locate/polymer

Quantifying the effects of contact duration, loading rate, and approach velocity on P-selectin–PSGL-1 interactions using AFM

Shouqin Lü [a,1], Zhiyi Ye [a,b,1], Cheng Zhu [c,*], Mian Long [a,*]

[a] National Microgravity Laboratory, Institute of Mechanics, Chinese Academy of Sciences, Beijing 100080, People's Republic of China
[b] College of Bioengineering, Chongqing University, Chongqing 400044, People's Republic of China
[c] Coulter Department of Biomedical Engineering, Georgia Institute of Technology, Atlanta, Georgia 30332, USA

Received 8 October 2005; received in revised form 14 November 2005; accepted 16 November 2005
Available online 15 February 2006

Abstract

Kinetics and its regulation by extrinsic physical factors govern selectin–ligand interactions that mediate tethering and rolling of circulating cells on the vessel wall under hemodynamic forces. While the force regulation of off-rate for dissociation of selectin–ligand bonds has been extensively studied, much less is known about how transport impacts the on-rate for association of these bonds and their stability. We used atomic force microscopy (AFM) to quantify how the contact duration, loading rate, and approach velocity affected kinetic rates and strength of bonds of P-selectin interacting with P-selectin glycoprotein ligand 1 (PSGL-1). We found a saturable relationship between the contact time and the rupture force, a biphasic relationship between the adhesion probability and the retraction velocity, a piece-wise linear relationship between the rupture force and the logarithm of the loading rate, and a threshold relationship between the approach velocity and the rupture force. These results provide new insights into how physical factors regulate receptor–ligand interactions.

Keywords: Adhesion probability; Rupture force; Kinetic rates

1. Introduction

Selectin–ligand interactions mediate the tethering and rolling of circulating cells on vascular surface, an initiating events of the multi-step adhesion and signaling process in inflammatory responses and tumor metastases [1–6]. There are three known members of the selectin family: P-, E-, and L-selectin. Their common structure includes an N-terminal, C-type lectin domain, followed by an epidermal growth factor like module, multiple copies of consensus repeat units characteristic of complement binding proteins, a transmembrane segment, and a short cytoplasmic domain [7,8]. P-selectin is expressed on activated endothelial cells and platelets and interacts with P-selectin glycoprotein ligand 1 (PSGL-1) [9,10], which is expressed on leukocytes. Both P-selectin and PSGL-1 have been well-characterized biochemically; as such, they provide an ideal system for investigating the biophysical factors that influence the kinetics of receptor–ligand interactions.

Receptor–ligand interactions are governed by reaction kinetics in which both on- and off-rates are important. Under physiological condition, P-selectin and PSGL-1 interact in two rather than three dimensions, as both molecules are anchored on the surfaces of two apposing cells. The kinetic rates of three-dimensional (3D) binding in the fluid phase likely reflect their intrinsic values. By comparison, not only is two-dimensional (2D) binding determined by their intrinsic association and dissociation rates but it also is influenced by various extrinsic physical factors. On the one hand, flowing cells in circulation are convected by the blood stream, which drives them to collide with the vascular surface. For the interacting molecules to dock, they have to first properly orient their binding pockets. Thus, on-rate depends on the relative velocity [11] and the separation distance [12] of the apposing surfaces as well as the surface presentation of the interacting molecules. Indeed, the orientation and length of the molecules and the micromorphology of the cell surface on which they are expressed affect the on-rate but not the off-rate of their interaction

* Corresponding authors. Tel./fax: +86 10 6261 3540 (M. Long)
Tel.: +1 404 894 3269; fax: +1 404 385 1397 (C. Zhu)
E-mail addresses: mlong@imech.ac.cn (M. Long), cheng.zhu@me.gatech.edu (C. Zhu).
[1] The authors have the equal contributions to the paper.

0032-3861/$ - see front matter © 2006 Published by Elsevier Ltd.
doi:10.1016/j.polymer.2005.11.095

[13,14]. The adhesion probability of the P-selectin–PSGL-1 interaction increases with the increasing velocity to separate the interacting molecules [15,16]. It has been proposed that more rapid and forceful approach of selectins toward their ligands can promote bond formation by providing the required velocity and force to overcome or penetrate a repulsive barrier [17]. This has been suggested as a mechanism for the counter-intuitive flow-enhanced adhesion [17], in which increasing flow promotes adhesion despite the fact that the dislodging forces are increased [18,19].

On the other hand, flow exerts hydrodynamic forces on the cells that must be balanced by adhesive forces on the receptor–ligand bonds, which regulate their dissociation. Thus, off-rates are regulated by externally applied force. Indeed, selectin–ligand interactions have served as a model system for the first intensive analysis of how off-rates depend on force [15,16,20–27] and on the history of force application [27]. Different types of bond behaviors have been defined: slip bonds dissociate more rapidly at higher forces than at lower forces, whereas catch bonds dissociate less rapidly at higher forces than at lower forces [28]. A simple model for the intuitive slip bonds is the Bell equation, which assumes that the off-rate increases exponentially with an increasing force [29]. When a ramp force is applied to break the bond, the force dependence of off-rate translates to the dependence of rupture force on the rate of force application, or loading rate [30]. The theory of dynamic force spectroscopy (DFS) predicts that the bond strength, defined as the most probable rupture force, increases linearly with the logarithm of loading rate [31,32]. Recently, P-selectin has been shown to form catch bonds at low forces and slip bonds at high forces with PSGL-1 [33]. To explain transitions between catch and slip bonds a two-pathway model has been proposed, which assumes the existence of two bound states that dissociate along two pathways with distinct sensitivity to force [16,34]. The potential presence of dual bound states may provide a possible mechanism for the velocity for the interacting molecules to approach each other to regulate the bond strength by biasing the proportions of the two bound states.

In the present work, we used atomic force microscopy (AFM) to study the influences of several physical factors on P-selectin–PSGL-1 interaction. These include the time during which the two molecules are allowed to interact, the velocity from which the two molecules separate, the rate at which force is applied to rupture the molecular bonds, and the velocity to which the two molecules approach. The impact of these physical factors on the P-selectin–PSGL-1 interaction is assessed by their effects on the adhesion frequency and on the rupture force, which are governed by on- and off-rates. Our results reveal a saturable relationship between the contact time and the rupture force, a biphasic relationship between the adhesion probability and the retraction velocity, a piece-wise linear relationship between the rupture force and the logarithm of the loading rate, and a threshold relationship between the approach velocity and the rupture force. These results provide new insights into how physical factors regulate P-selectin–PSGL-1 interactions.

2. Experimental procedures

2.1. Proteins and antibodies

Soluble P-selectin (sPs) consisting of entire extracellular domain [8], anti-P-selectin capturing (S12) and blocking (G1) monoclonal antibodies (mAbs) (mIgG1) [35], and anti-PSGL-1 blocking mAb PL1 (mIgG1) [36] were generous gifts from Dr Rodger P. McEver (Oklahoma Medical Research Foundation). Membrane-anchored PSGL-1 (mPSGL-1) molecules were purified from human neutrophils using an affinity chromatography procedure [35]. Bovine serum albumin (BSA) was purchased from Sigma Chemical Co. (St Louis, MO).

2.2. Functionalizing the AFM

A previously described protocol [23,33] was used to couple the interacting molecules onto AFM tips and mica surfaces. Briefly, capturing mAb S12 were adsorbed onto cantilever tip by incubating the cantilever at 4 °C overnight in a 10 μg/ml protein solution. The cantilever was washed and blocked by 1% BSA in Hanks' balanced salt solution (HBSS). The washed cantilever was then incubated in a 1 μg/ml soluble sPs solution for 30 min to allow the sPs molecules to be captured in a proper orientation (Fig. 1(b)). Purified mPSGL-1 molecules were incorporated in lipid vesicles and then reconstituted by vesicle fusion in a polyethylenimine (PEI) polymer-supported lipid bilayer onto mica surface [23,33,37]. PSGL-1 bilayer was used immediately and AFM experiments were done in HBSS containing 1% BSA (Fig. 1(b)).

2.3. AFM assay

A NanoScopeIV MultiMode PicoForce AFM (Digital Instruments, Santa Barbara, CA) was used to measure the adhesions and dissociations of P-selectin–PSGL-1 interactions (Fig. 1(a)). The instrument was housed in a temperature-controlled room (~19 °C) with little temperature fluctuation. Commercial cantilevers were used (™Microscopes, Sunnyvale, CA). The cantilever spring constants k_c, which ranges from 5 to 13 pN/nm (cantilever C) and 32 to 38 pN/nm (cantilever D), were calibrated in situ for each cantilever by thermal fluctuation analysis using a software provided by the manufacturer. The PSGL-1-reconstituted lipid bilayer was placed on the AFM stage, which was repeatedly driven to approach the sPs-coated cantilever tip, to make contact at a compressive force of ~50 pN to allow reversible bond formation and dissociation, and to retract away to allow observation of the adhesion event and measurement of rupture force, if any. The approach velocity, contact duration, and retraction velocity were varied separately in different experiments, while the contact force was kept nearly constant. The adhesion and force signals for each approach-contact-retract cycle were collected from a quad photodetector (Fig. 1(c)). At least three different locations on each lipid bilayer were tested for 150–400 cycles at each location to collect a set of adhesion events and rupture forces. All experiments were repeated at

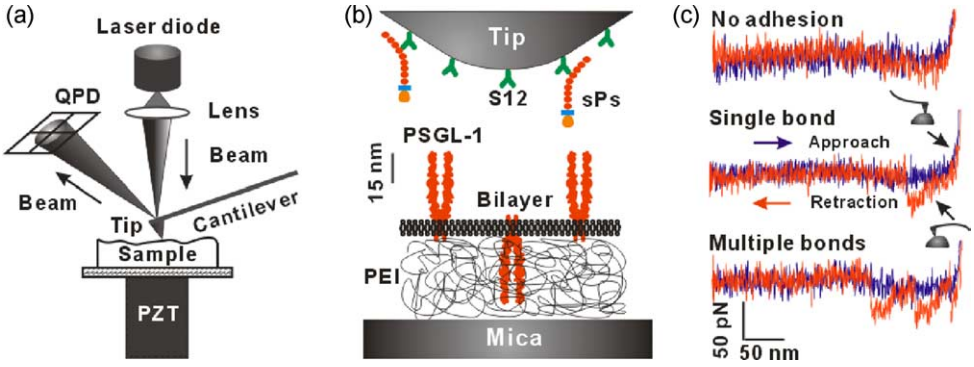

Fig. 1. AFM system. (a) Schematic of AFM instrument. A piezoelectric translator (PZT) was used to drive the movement of PSGL-1-incorporated bilayer. Adhesion and force signal were collected from a quad photodetector (QPD), which measured the laser reflected on the back of the cantilever. (b) Functionalizing AFM tip. Soluble P-selectin was captured by its non-blocking mAb S12 pre-adsorbed on the AFM tip. PSGL-1 was reconstituted in a lipid bilayer supported by a PEI-cushioned mica. (c) Force–displacement curves. PSGL-1-incorporated bilayer was driven to approach to (from left to right), contact with, and retract from (from right to left) sPs-coated AFM tip. Adhesion was visualized from the cantilever deflection and rupture force was measured from the force–displacement curve (middle and lower panels).

least three times. Low molecular densities were used to achieve infrequent binding (<35%).

During the fast retraction of the AFM stage the cantilever was bent by the viscous drag in addition to the adhesion force of the P-selectin–PSGL-1 bond. The adhesion force acted at the tip of the cantilever and vanished as soon as the P-selectin–PSGL-1 bond ruptured, while the viscous drag acted at the entire cantilever body and would only diminish after the stage stopped and the cantilever sprung back. Rupture force, f, of an adhesion event was determined by multiplying the cantilever spring constant, k_c, by the drop in cantilever deflection, Δz, measured from the photodetector during the brief interval of the rupture event while the stage continued to retract. Hence the viscous drag, which continued to bend the cantilever, was excluded from the rupture force determination [27,42].

In addition to bending the AFM cantilever, the force acting on the P-selectin–PSGL-1 complex also stretched the molecules. Since the extent of this stretch increased with increasing force, the molecular spring has to be taken into account in the calculation of the loading rate. We have recently shown that P-selectin–PSGL-1 complex behaves as a nearly linear spring with a spring constant of $k_m = 1$ pN/nm [43]. Hence, the loading rate was calculated as the product of retraction velocity, v_r, and system spring constant, $k_s = k_c k_m/(k_c + k_m)$ since the cantilever spring and the molecular spring are in serial arrangement during stretch [43]. Alternatively, the system spring constants could be directly measured from the slope of the nearly linear force–displacement curve since the stage displacement equals the sum of the cantilever deflection and the molecular extension.

2.4. Data analysis

A previously described mathematical model was used to predict the dependence of the probabilities of adhesion, P_a, and of double bonds, p_2, on contact duration t and to estimate the kinetic parameters [13,14,38–41]

$$P_a(t) = 1 - \exp\{-m_r m_l A_c K_a^0 [1 - \exp(-k_r^0 t)]\} \quad (1)$$

$$p_2(t) = \exp\{-m_r m_l A_c K_a^0 [1 - \exp(-k_r^0 t)]\} \times \{-m_r m_l A_c K_a^0 [1 - \exp(-k_r^0 t)]\}^2/2! \quad (2)$$

where, k_r^0 and K_a^0 are the zero-force reverse rate and binding affinity, m_r and m_l are the site densities of receptors and ligands, respectively, and A_c is the contact area. The fraction of double bonds in all adhesion events can be calculated from Eqs. (1) and (2):

$$F_2 = p_2/P_a = 1/2(1 - P_a)\ln^2(1 - P_a)/P_a \quad (3)$$

The measured binding curves of frequencies of adhesion and of double rupture events versus contact duration were respectively fit to Eqs. (1) and (2) to calculate two sets of reverse rate, k_r^0, and lumped surface binding affinity, $m_r m_l A_c K_a^0$, which were then compared to each other. For experiments in which the frequencies of adhesion and of double rupture events were measured in a single contact duration of 1 s only, Eq. (3) was used to predict the fraction of double bonds from the measured adhesion frequency, and then compared to the measured fraction of double rupture events.

Dynamic force spectroscopy (DFS) analysis was used to predict the dependence of rupture forces on loading rates. It is assumed that the P-selectin–PSGL-1 bond follows the first-order irreversible dissociation kinetics. The reserve rate, k_r, is assumed to be an exponential function of applied force, f [29]

$$k_r(f) = k_r^0 \exp(af/k_B T) \quad (4)$$

where k_B is the Boltzmann constant and T is the absolute temperature, and a is the so-called reactive compliance, which measures the width of the energy well that kinetically traps the interacting molecules in the bound state. Assuming that the reverse rate k_r depends on time t through the force f, which is equal to the loading rate r_f times t, it follows that the most probable rupture force or peak force, f_m, versus $\ln(r_f)$ should be a straight line [30,32],

$$f_m = \frac{k_B T}{a}\ln(r_f) - \frac{k_B T}{a}\ln\left(\frac{k_r^0 k_B T}{a}\right) \quad (5)$$

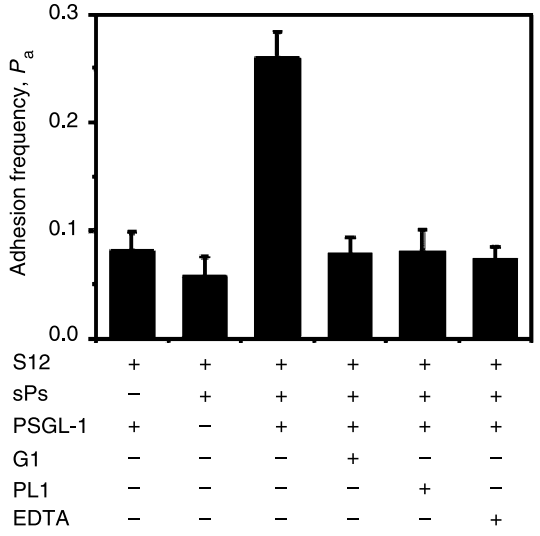

Fig. 2. Binding specificity. sPs-coated tip adhered to PSGL-1-incorporated bilayer with 20–30% frequencies at contact time $t=1$ s, and the approach and retraction velocities of $v_a=v_r=1000$ nm/s. Adhesion was much less frequent when tips adsorbed with S12 only contacted PSGL-1-incorporated bilayer or when sPs-coated tip contacted plain bilayer. Adhesion was also blocked by anti-P-selectin mAb G1 or anti-PSGL-1 mAb PL1, and by inclusion of the calcium chelator EDTA in the media. Data were presented as the mean ± standard error of adhesion probability, P_a.

Two line segments in the f_m versus $\ln(r_f)$ plot are interpreted as two Bell models in series

$$(k_r)^{-1} = \sum_{i=1}^{2} [k_i^0 \exp(a_i f/k_B T)]^{-1} \quad (6)$$

which can be fitted by

$$(r_f)^{-1} = \sum_{i=1}^{2} [(k_i^0 k_B T/a_i)\exp(a_i f_m/k_B T)]^{-1} \quad (7)$$

to yield two sets of Bell model parameters (k_i^0, a_i) ($i=1$, 2) [22,27].

3. Results

3.1. Binding specificity

Adhesive events were visualized from the photodiode signals that monitored the cantilever deflections (Fig. 1(c)). Binding was quantified by the adhesion probability, P_a, defined as the fraction of adhesive events resulted from a total of >200 test cycles. In the control experiments, P_a was measured at contact time $t=1$ s at the same approach and retraction velocities of $v_a=v_r=1000$ nm/s. Twenty to thirty percent of P_a was observed when sPs-coated tips contacted PSGL-1-incorporated lipid bilayers but it was reduced to 5–10% when AFM tips coated with S12 only contacted PSGL-1-incorporated bilayers or when sPs-coated tips contacted plain bilayers. Adhesion was also blocked by anti-P-selectin mAb G1 or anti-PSGL-1 mAb PL1, and abrogated by the calcium chelator EDTA (Fig. 2). These data, together with the similar data at various contact times (Fig. 3(a) comparing the solid squares and solid triangles), demonstrated that the observed adhesion was mediated predominately by the specific interactions between P-selectin–PSGL-1 molecules. Importantly, not only were the nonspecific adhesions much less frequent but they also did not contribute disproportionately to the force data, because their values were no larger than the specific forces (data not shown).

3.2. Dependence of contact duration

Dependence of adhesion frequency on contact duration was measured at contact times ranging from 0.05 to 5 s at the same approach and retraction velocities of $v_a=v_r=1000$ nm/s. The specific adhesion probability, P_a, was obtained by removing the nonspecific adhesion frequency (solid triangles and fitted dashed line in Fig. 3(a), left ordinate), from the directly measured total adhesion frequency, as it was previously done in the micropipette assay [13,14,38–41]. As shown in Fig. 3(a), the data (solid squares, left ordinate) exhibit a transient phase where P_a increased with t and a steady phase where P_a reached equilibrium. The measured P_a curve was well fitted by Eq. (1)

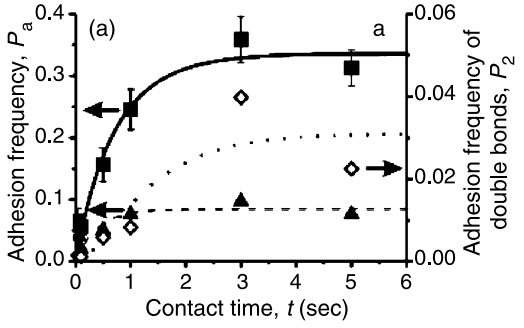

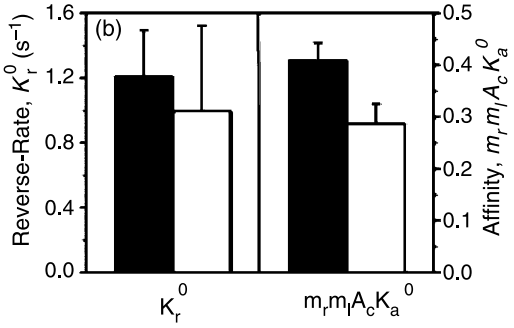

Fig. 3. Dependence of probabilities of adhesion and of double rupture events on contact duration. (a) Dependence of adhesion probability (solid squares, left ordinate), presented as the mean ± standard error of adhesion probability in at least five independent measurements, was fitted by Eq. (1) (solid curve, left ordinate). The dependence of double rupture event probability (open diamonds, right ordinate) was fitted by Eq. (2) (dot line, right ordinate). Also plotted are the data for non-specific adhesions (solid triangles, left ordinate), and the predicted nonspecific binding by fitting Eq. (1) to the nonspecific data (dashed line, left ordinate). The approach and retraction velocities were $v_a=v_r=1000$ nm/s. (b) Comparison of reverse rate k_r^0 (left ordinate) and lumped surface binding affinity $m_r m_l A_c K_a^0$ (left ordinate) predicted from adhesion probability data (solid bars) with their counterparts predicted from the data of double rupture event probability (open bars).

(solid curve), which returns two parameters: $k_r^0 = 1.21 \pm 0.28\ s^{-1}$ and $m_r m_l A_c K_a^0 = 0.41 \pm 0.03$ (solid bars in Fig. 3(b)).

A small fraction of the adhesive events displayed two rupture events in the force–extension curves (cf. lowest panel in Fig. 1(c)). The frequency p_2 of double-rupture events (open diamonds in Fig. 3(a), right ordinate) followed a time course similar to that of $P_a(t)$, which can be fitted by Eq. (2) (dot curve). It is evident that the kinetic parameters obtained from fitting Eq. (2) to the p_2 data ($k_r^0 = 1.00 \pm 0.53\ s^{-1}$ and $m_r m_l A_c K_a^0 = 0.29 \pm 0.04$, open bars in Fig. 3(b)) are consistent with the corresponding parameters estimated from fitting Eq. (1) to the P_a data (solid bars in Fig. 3(b)).

Dependence of rupture force on contact duration was also measured at the above contact times. The histogram of rupture forces exhibits a single peak at each contact time (Fig. 4(a)). The most probable rupture force, f_m (open triangles), followed time curve very similar to those of the $P_a(t)$ and $p_2(t)$, increasing initially but reaching a plateau thereafter (Fig. 4(b)). Indeed, plotting f_m against the average number of bonds, $\langle n \rangle = -\ln(1 - P_a)$, revealed a strong correlation (Fig. 4(c)). It is therefore possible that the changes in f_m are caused by the changes in the number of bonds. Alternatively, longer contact between P-selectin and PSGL-1 may promote formation of stronger bonds.

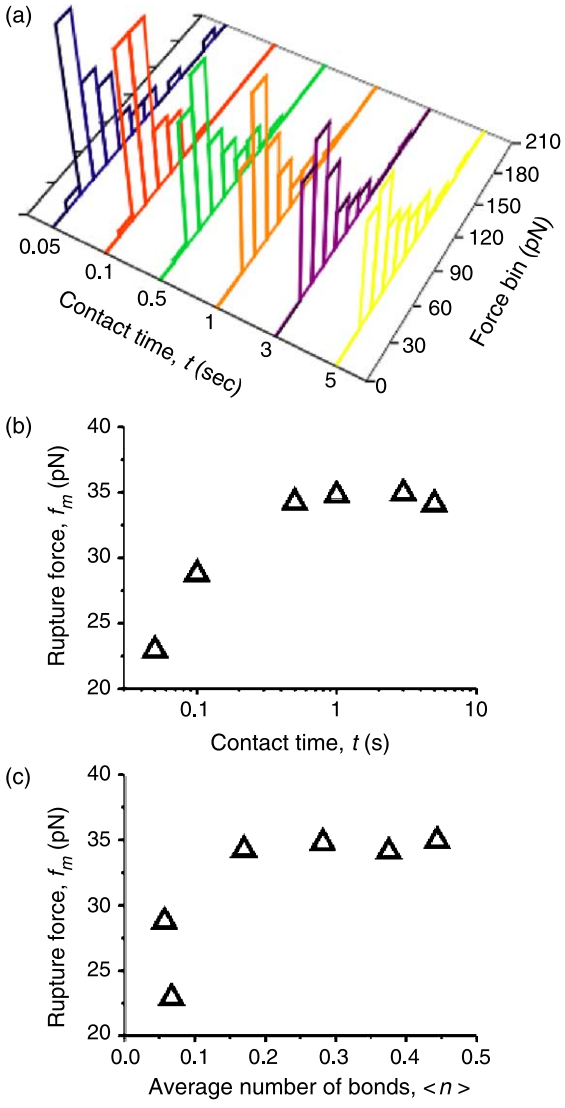

Fig. 4. Dependence of rupture force on contact duration. (a) Histograms of rupture forces measured at the indicated contact durations. Total of >100 forces at each contact time (except at $t = 0.05$ s, which had ~50 forces) were collected and analyzed by histogram of bin size of 15 pN. (b) Dependence of the most probable rupture force, f_m (open triangles), on contact durations. (c) Correlation between most probable force f_m and average number of bonds, $\langle n \rangle = -\ln(1 - P_a)$, calculated from Eq. (1) [38]. The approach and retraction velocities were $v_a = v_r = 1000$ nm/s.

3.3. Dependence of cantilever retraction velocity/force loading rate

Transport has been suggested to affect tethering of flowing cells to the vascular surface, as binding can be decomposed into a two-step process with one step of transport that brings the interacting molecules in close proximity followed by the other step of intrinsic molecular docking [11,44]. To assess the transport effects we measured the dependence of adhesion frequency on the cantilever retraction velocity in the range from $v_r = 100$–$34{,}900$ nm/s at a given approach velocity of $v_a = 1000$ nm/s and a given contact time of $t = 1$ s. The adhesion probability increased initially with the retraction velocity, reached a maximum around $v_r \sim 4190$ nm/s ($P_{a,max} = 0.29$), and decreased thereafter (Fig. 5).

We next measured the dependence of rupture force on loading rate in the range from 0.13 to 45.6×10^3 pN/s. The histogram of rupture forces at each loading rate exhibited a prominent peak that shifted rightwards with increasing loading rates (Fig. 6(a)). To perform DFS analysis, we plotted the most probable force, f_m, against $\log(r_f)$ (solid triangles in Fig. 6(b)). These plots show a continuous curve that is well fitted by the model in Eq. (7) (solid line in Fig. 6(b)), which is similar to our previous data (open circles in Fig. 6(b)) [27]. The kinetic parameters so obtained, $k_1^0 = 0.91\ s^{-1}$ and $a_1 = 7.20$ Å; $k_2^0 = 48.67\ s^{-1}$, $a_2 = 0.73$ Å, are also comparable with the previously reported values [27].

Fig. 5. Dependence of adhesion probability on retraction velocity. The approach velocity was $v_a = 1000$ nm/s and the contact time was $t = 1$ s. Data were presented as the mean ± standard error of adhesion probability of at least three independent measurements.

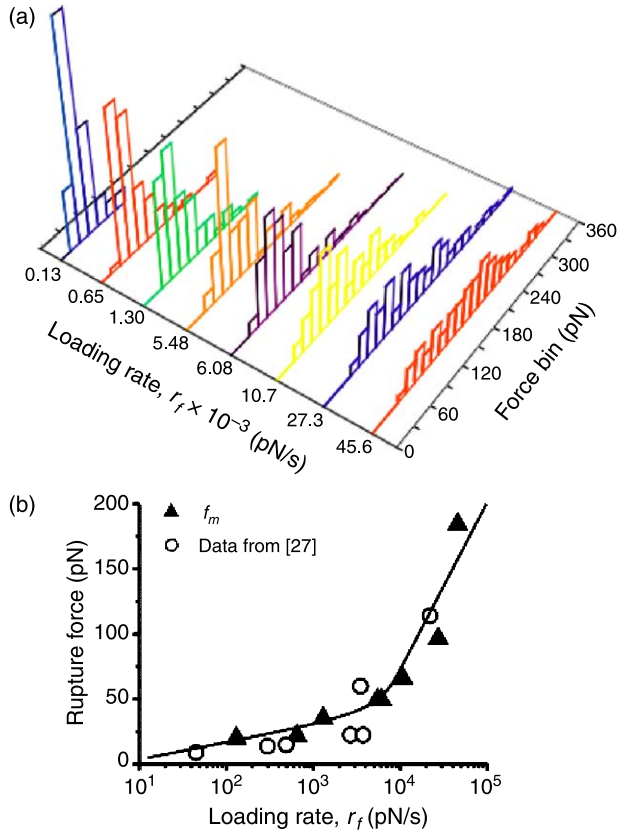

Fig. 6. Dependence of rupture force on loading rate. (a) Histograms of rupture forces at various loading rates. Total of >120 forces at each loading rate (except at $r_f = 4.56 \times 10^4$ pN/s, which had ~70 forces) were collected and analyzed by histogram of a force bin of 15 pN. (b) Dependence of the most probable force, f_m, on loading rates. The measured f_m data (solid triangles) were fitted by Eq. (7) (solid line). The best-fit Bell parameters were $k_1^0 = 0.91\ s^{-1}$, $a_1 = 7.20$ Å; $k_2^0 = 48.67\ s^{-1}$, $a_2 = 0.73$ Å. Also plotted are the data from reference [27] (open circles). The approach velocity was $v_a = 1000$ nm/s and the contact time was $t = 1$ s.

3.4. Dependence of approach velocity

The effects of transport were also assessed by quantifying the dependence of adhesion frequency on approach velocity, which was measured in a range from $v_a = 100$–34,900 nm/s at a given retraction velocity of $v_r = 1000$ nm/s and a given contact time of $t = 1$ s. The adhesion probability P_a (solid squares in Fig. 7, left ordinate) was found to be indifferent to the approach velocity in the range tested. Furthermore, the measured fraction of double rupture events, F_2, is again indifferent to the approach velocity (open circles in Fig. 7, right ordinate), which are consistent with the F_2 values predicted from the measured P_a values using Eq. (3) (open triangles in Fig. 7, right ordinate). Thus, the same number bonds were formed with the same likelihood regardless of the approach velocity.

Remarkably, the rupture force histograms measured at low approach velocities were quite similar but rightward shifted gradually towards higher forces as approach velocity increased beyond 14,000 nm/s (Fig. 8(a)). The plots of the most probable forces f_m (open triangles) versus approach velocity showed more obvious trend (Fig. 8(b)). To relate the increased bond

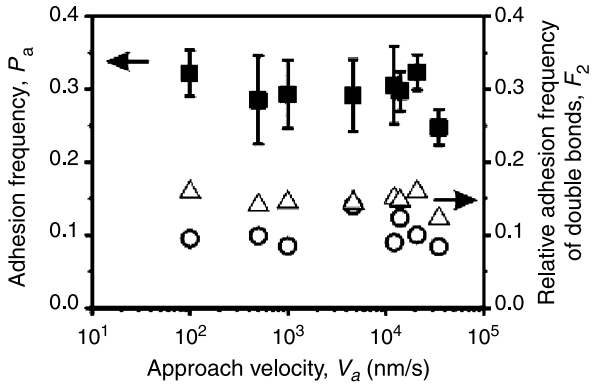

Fig. 7. Dependence of adhesion probability (solid squares, left ordinate) on approach velocity. Data were presented as the mean ± standard error of adhesion probability of at least three independent measurements. Also plotted are the measured fractions of double rupture events (open circles, right ordinate) and those predicted from the adhesion probabilities using Eq. (3) (open triangles, right ordinate). The retraction velocity was $v_r = 1000$ nm/s and the contact time was $t = 1$ s.

strength to the decreased bond dissociation rate, the probability density function predicted from the Bell equation, $p(y) = \exp[y - \exp(y) + 1]$ where $y = af/k_BT - \ln[(r_f a)/(k_B T k_r^0)]$, was fit to the prominent peak in each rupture force histograms (Fig. 8(a)) to evaluate the Bell model parameters for that approach velocity [16], which are shown in Fig. 8(c). It is evident from Fig. 8(a) that this asymmetric function fits the measured rupture force distributions reasonably well. However, the data are generally more broadly distributed (Fig. 8(a)) than those predicted by this equation, as are most of the published data in the literature [45]. Possible reasons for this discrepancy may include the more complex force- and force history-dependence of off-rate than the oversimplified Bell model can describe [27], possible contamination of multiple bonds, and experimental errors. Remarkably, the zero-force off-rate exhibits a threshold behavior, which was insensitive to the approach velocity below 14,000 nm/s but decreased sharply with increasing approach velocity thereafter (solid squares in Fig. 8(c), left ordinate). By comparison, the reactive compliance a appeared to be insensitive to the approach velocity (open circles in Fig. 8(c), right ordinate). These data suggest that more rapid and forceful collision between P-selectin and PSGL-1 beyond a threshold promotes formation of stronger and longer-lived bonds.

4. Discussions and conclusions

Kinetics and its regulation by extrinsic physical factors govern selectin–ligand interactions that mediate tethering and rolling of circulating cells on the vessel wall under hemodynamic forces. While the force regulation of off-rate for dissociation of selectin–ligand bonds has been extensively studied, much less is known about how transport impacts the on-rate for association of these bonds and their stability. In the present study, the probabilities of adhesion and of double bonds were used to assess the on-rate. The rupture forces were used to assess the off-rate and the bond stability. The

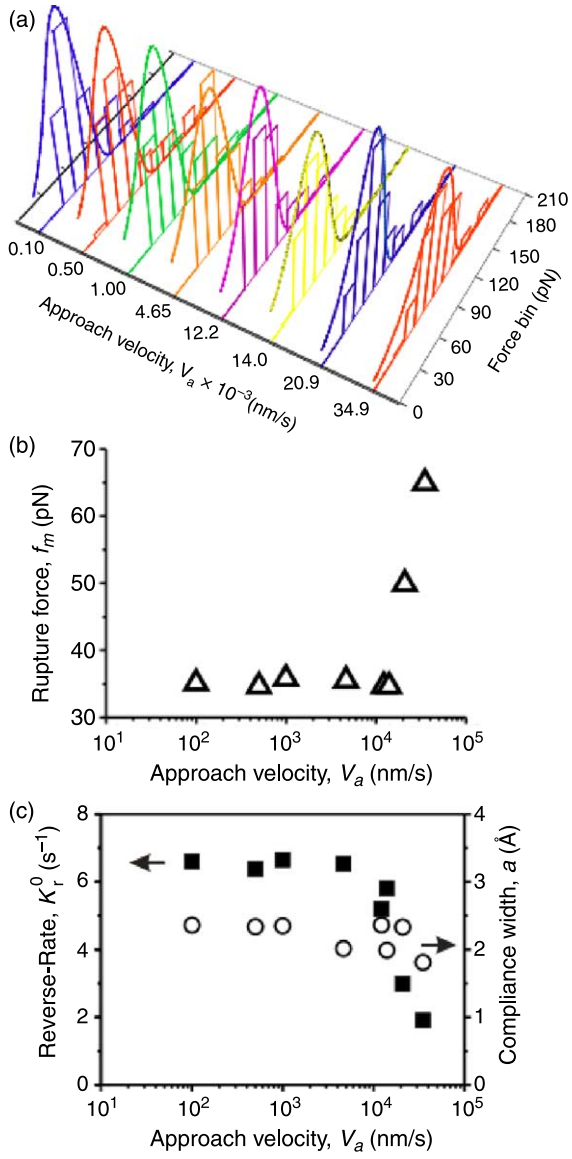

Fig. 8. Dependence of rupture force on approach velocity. (a) Histograms of rupture forces measured at the indicated approach velocities. Total of >90 force values at each approach velocity were collected and analyzed by histogram of a force bin of 15 pN, and compared with the predictions (curves) from the Bell model (cf. text). (b) Dependence of the most probable force, f_m (open triangles, left ordinate), on approach velocities. (c) Dependence of reverse rate k_r^0 (solid squares) and reactive compliance a (open circles, right ordinate) on approach velocities. These parameters were calculated from fitting the probability density function predicted by the Bell model to the measured of rupture force histograms as described in the text. The retraction velocity was $v_r = 1000$ nm/s and the contact time was $t = 1$ s.

dependence of these matrices of on- and off-rates on the contact duration, retraction velocity/loading rate, and approach velocity were quantified. Our results contribute to the understanding of how selectin–ligand interactions are regulated by physical factors.

The dependence of the adhesion probability on the contact time is well fitted by a previously described probabilistic model (Eq. (1)) [38]. The validity of this model has been supported in previous studies using micropipette [13,14,38–41,46] and laser tweezers [47]. The present study has provided further support to this model. This is expected, because although a different technique—AFM—was used to measure adhesion, it was the same adhesion frequency assay to which the model is applied. The off-rate obtained in this study is in good agreement with the values previously measured with the micropipette using PSGL-1-expressing HL-60 cells interacting with P-selectin-coated red blood cells [13,48]. Direct comparison between values of the effective affinities $A_c K_a^0$ measured from the present and previous experiments is not possible because the respective site densities of PSGL-1 in the bilayer and of P-selectin on the AFM tips were not available. Similar to the previous study [41], additional data of multiple rupture events were used to further test a prediction of the model (Fig. 3(a)). Both values of k_r^0 *and* $m_r m_l A_c K_a^0$ evaluated from the adhesion probability data compare reasonably well with their counterparts evaluated from the data of double rupture events. The slightly lower $m_r m_l A_c K_a^0$ value predicted from the p_2 data than that predicted from the P_a data (Fig. 3(b)) suggests that some of the double bond dissociation events might not give rise to double-peaks clearly resolvable in the force scan curves. This hypothesis is supported by the slightly lower fractions of double rupture events measured directly than those predicted from the measured adhesion frequencies (Fig. 7). Thus, the favorable comparison attests to the reliability of these parameters. It also argues that the individually observed rupture events represent dissociation of single bonds that follow a Poisson distribution, an underlying assumption of Eqs. (1)–(3).

The DFS analysis of the rupture forces yielded a force spectrum—a plot of the most probable rupture force versus the logarithm of loading rate—very similar to that of a previous study [27]. Although the same P-selectin–PSGL-1 interaction was studied, the two sets of data were obtained from two laboratories using different instruments and reagents. Furthermore, the interacting molecules were functionalized in two different ways in the AFM. The previous study used soluble PSGL-1-coated AFM tips to interact with membrane P-selectin-incorporated bilayers [27]. The present work used an inverted configuration, i.e. soluble P-selectin-coated AFM tips interacting with membrane PSGL-1-incorporated bilayers (Fig. 1(b)). The reasonable agreement between the two studies imparts confident in our data. P-selectin–PSGL-1 interactions have been shown to behave as catch–slip transitional bonds [33]. However, we were unable to detect the presence of catch bonds in the low force regime from the analysis of histograms of rupture forces measured from the constant-rate steady-ramp experiment. This discrepancy has been explained by the force-history dependence of off-rates [27]. Lifetime measurement at various levels of constant force was not possible in the present study because the force in the commercial AFM used could not be held constant at low levels where catch bonds were expected [16,33].

A major goal of the present study is to quantify the effects of transport on bond formation. To mimic the convective transport of the interacting molecules by the moving cell, the velocities of the P-selectin bearing AFM tips approach to and retraction from the PSGL-1 bilayers were systematically

varied. A biphasic dependence of the adhesion probability on the retraction velocity was found. This cannot be explained by the increase in bond strength with increasing loading rate, which potentially could have reduced the number of weak binding events that might have failed to be detected. The reason is that such an effect would have yielded a monotonically increasing curve rather than a biphasic curve. Instead, our data are consistent with the published tethering frequency versus wall shear rate data [44]. In that study, the frequency of PSGL-1-expressing neutrophils tethering to P-selectin coated on a flow chamber floor was shown to depend biphasically on the wall shear rate.

Perhaps the most interesting finding of the present study is the effects of approach velocity. The mechanical strength and zero-force off-rate of the P-selectin–PSGL-1 bonds were insensitive to the approach velocity when it was below 14,000 nm/s, but increased and decreased sharply with further increase in the approach velocity, respectively (Fig. 8(b) and (c)). By comparison, the adhesion probability and reactive compliance were found to be indifferent to the approach velocity (Figs. 7 and 8(c)). Note that the time during which the P-selectin approached the PSGL-1 (which is inversely proportional to the approach velocity) is negligibly small compared to the 1 s contact time during which the AFM tip was pressed on the bilayer with a constant force. Thus, on-rate of bond formation is not affected by the approach velocity. However, the bonds formed with more rapid approach exhibit greater strength (Fig. 8(b)) and slower zero-force off-rate (Fig. 8(c)). P-selectin–PSGL-1 interactions have been modeled as having two bound states to explain their catch–slip transitional bond behavior [16,34]. At zero force it dissociates rapidly from one bound state but slowly from the other bound state. A possible explanation for our data may be that fast approach velocity favors bond formation in the slow dissociating bound state. It has been proposed that more rapid and forceful approach of selectins toward their ligands can promote bond formation by providing the required velocity and force to overcome or penetrate a repulsive barrier [17]. Our result seems to support an alternative hypothesis. It is not more bonds, but stronger and longer-lived bonds that are promoted by the more rapid and forceful approach. In spite of the difference, this alternative hypothesis may still provide a possible mechanism for flow-enhanced adhesion.

Acknowledgements

We thank Dr R.P. McEver for the generous gifts of sPs, S12, G1 and PL1 proteins, Drs J.G. Geng and L Li for PSGL-1 purification. We also thank Dr C.T. Lim from the Division of Bioengineering, National University of Singapore for AFM instrument support and useful discussions, and A. Li for technical assistances. This work was supported by NSFC grants 10332060, 30225027, and 10128205, a CAS grant KJCX2-SW-L06 (ML) and a CAS OOSA grant 2005-1-16 (CZ and ML), NIH grant AI44902 (CZ) and TW 05774-01 (CZ and ML).

References

[1] Springer TA. Nature 1990;346:425–34.
[2] Springer TA. Cell 1994;76:301–14.
[3] Vestweber D, Blanks JE. Physiol Rev 1999;79:181–213.
[4] McEver RP. Thromb Haemost 2001;86:746–56.
[5] McEver RP. Curr Opin Cell Biol 2002;14:581–6.
[6] Lawrence MB, Springer TA. Cell 1991;65:859–73.
[7] Ley K, Gaehtgens P, Fennie C, Singer MS, Lasky LA, Rosen SD. Blood 1991;77:2553–5.
[8] Ushiyama S, Laue TM, Moore KL, Erickson HP, McEver RP. J Biol Chem 1993;268:15229–37.
[9] Moore KL, Stults NL, Diaz S, Smith DF, Cummings RD, Varki A, et al. J Cell Biol 1992;118:445–56.
[10] Li F, Erickson HP, James JA, Moore KL, Cummings RD, McEver RP. J Biol Chem 1996;271:6342–8.
[11] Chang KC, Hammer DA. Biophys J 2000;79:1891–902.
[12] Pierres A, Feracci H, Delmas V, Benoliel AM, Thiery JP, Bongrand P. Proc Natl Acad Sci USA 1998;95:9256–61.
[13] Huang J, Chen J, Chesla SE, Yago T, Mehta P, McEver RP, et al. J Biol Chem 2004;279:44915–23.
[14] Williams TE, Nagarajan S, Selvaraj P, Zhu C. J Biol Chem 2001;276:13283–8.
[15] Fritz J, Katopodis AG, Kolbinger F, Anselmetti D. Proc Natl Acad Sci USA 1998;95:12283–8.
[16] Evans E, Leung A, Heinrich V, Zhu C. Proc Natl Acad Sci USA 2004;101:11281–6.
[17] Chen S, Springer TA. J Cell Biol 1999;144:185–200.
[18] Finger EB, Puri KD, Alon R, Lawrence MB, von Andrian UH, Springer TA. Nature 1996;379:266–9.
[19] Lawrence MB, Kansas GS, Kunkel EJ, Ley K. J Cell Biol 1997;136:717–27.
[20] Alon R, Chen S, Puri KD, Finger EB, Springer TA. J Cell Biol 1997;138:1169–80.
[21] Alon R, Hammer DA, Springer TA. Nature 1995;374:539–42.
[22] Evans E, Leung A, Hammer D, Simon S. Proc Natl Acad Sci USA 2001;98:3784–9.
[23] Sarangapani KK, Yago T, Klopocki AG, Lawrence MB, Fieger CB, Rosen SD, et al. J Biol Chem 2004;279:2291–8.
[24] Hanley W, McCarty O, Jadhav S, Tseng Y, Wirtz D, Konstantopoulos K. J Biol Chem 2003;278:10556–61.
[25] Rinko LJ, Lawrence MB, Guilford WH. Biophys J 2004;86:544–54.
[26] Zhang XH, Bogorin DF, Moy VT. ChemPhysChem 2004;5:175–82.
[27] Marshall BT, Sarangapani KK, Lou JZ, McEver RP, Zhu C. Biophys J 2005;88:1458–66.
[28] Dembo M, Tourney DC, Saxman K, Hammer D. Proc R Soc London 1988;234:55–83.
[29] Bell GI. Science 1978;200:618–27.
[30] Evans E, Ritchie K. Biophys J 1997;74:1541–55.
[31] Merkel R, Nassoy P, Leung A, Ritchie K, Evans E. Nature London 1999;397:50–3.
[32] Zhu C. J Biomech 2000;33:23–33.
[33] Marshall BT, Long M, Piper JW, Yago T, McEver RP, Zhu C. Nature 2003;423:190–3.
[34] Barsegov V, Thirumalai D. Proc Natl Acad Sci USA 2005;102:1835–9.
[35] Geng JG, Bevilacqua M, Moore KL, McIntyre TM, Prescott SM, Kim JM, et al. Nature 1990;343:757–60.
[36] Moore KL, Patel KD, Bruehl RE, Fugang L, Johnson DA, Lichenstein HS, et al. J Cell Biol 1995;128:661–71.
[37] McConnell HM, Watts TH, Weis RM, Brian AA. Biochim Biophys Acta 1986;864:95–106.
[38] Chesla SE, Selvaraj P, Zhu C. Biophys J 1998;75:1553–72.
[39] Williams TE, Selvaraj P, Zhu C. Biophys J 2000;79:1858–66.
[40] Chesla SE, Li P, Nagarajan S, Selvaraj P, Zhu C. J Biol Chem 2000;275:10235–46.

[41] Long M, Zhao H, Huang KS, Zhu C. Ann Biomed Eng 2001;29: 935–46.
[42] Marshall BT, PhD Dissertation, Georgia Institute of Technology 2002.
[43] Marshall BT, Sarangapani KK, Wu JH, Lawrence MB, Rodger P, Zhu C. Biophys J 2005;90:681–92.
[44] Chen S, Springer TA. Proc Natl Acad Sci USA 2001;98:950–5.
[45] Zhu C, Lou J, McEver RP. Biorheology 2005;42:443–62.
[46] Williams TE, Nagarajan S, Selvaraj P, Zhu C. Biophys J 2000;79:1867–75.
[47] Thoumine O, Kocian P, Kottelat A, Meister JJ. Eur Biophys J 2000;29: 398–408.
[48] Zhu C, Long M, Chesla SE, Bongrand P. Ann Biomed Eng 2002;30: 305–14.